Molecular Exchange in Thermal Equilibrium Between Dissolved and Crystalline Tripalmitin by NMR

Negin Löfborg[a], Paul Smith[a,*], Istvan Furó[b], and Björn Bergenståhl[c]

[a]YKI, Institute for Surface Chemistry, SE-114 86 Stockholm, Sweden, [b]Division of Physical Chemistry, Department of Chemistry, Royal Institute of Technology, SE-100 44 Stockholm, Sweden, and [c]Department of Food Technology, Lund University, SE-221 00 Lund, Sweden

ABSTRACT: An NMR technique to measure exchange kinetics at thermal equilibrium in dispersions of moderately soluble crystalline material is presented. By monitoring the exchange of molecules between pools in solid and dissolved form, one can characterize the surface specific exchange rate. Illustrative experiments were performed in a model system with β-type crystals of tripalmitin as the solid phase and tripalmitin, a fraction of it deuterated, dissolved in a medium-chain TG oil as the liquid phase. The concentration of deuterated tripalmitin in the solvent was followed by ^{2}H NMR after the crystals, which initially lack deuterated tripalmitin, were immersed in the liquid. The variation of the ^{2}H concentration in the solvent provided the surface specific exchange rate. No systematic errors, due to the slight difference in properties of the deuterated tripalmitin compared to hydrogenated tripalmitin, were observed. The methodology worked well between crystal concentrations of 2 and 4 wt%.

Paper no. J10687 in *JAOCS 80,* 1187–1192 (December 2003).

KEY WORDS: Colloid chemistry, deuterium NMR dispersion, surface chemistry, surface exchange, triglyceride.

Molecular or atomic crystallization or dissolution rates are relatively easy to measure in systems that are out of thermal equilibrium, e.g., by exhibiting a concentration or a chemical potential gradient. In contrast, exchange between different phases of the same molecular species under conditions of thermal equilibrium has drawn significantly less attention. This type of exchange can be imagined as molecular diffusion in and out over a phase boundary between two phases in equilibrium. In a suspension, this exchange is most pronounced at the outermost atomic/molecular layers of the solid particles involved, although there also may be an exchange between the inner and outer molecular layers. Hence, diffusion in and out of the solid phase predominantly represents solidification and dissolution of molecules on/from the solid–liquid interface, respectively.

The exchange between solution and solid phase determines the rate of destabilization in systems with metastable compound solid phases. One example of such an exchange is TAG (fat) systems where several metastable and stable structures may exist, as exemplified by the cacao butter model recently reviewed by Sato *et al*. (1). Those authors identified several compound structures whose changing composition allows the formation of more stable forms. Hence, molecular exchange can strongly influence the kinetics of cacao butter and, in general, fat recrystallization.

In general, exchange experiments performed at thermal equilibrium require marking the molecules by particular isotopes of the constituting atoms. Thereafter, the marked molecules or atoms can be followed by isotope-selective techniques such as radiochemical methods or NMR spectroscopy. If, as usual, one can assume that the marker isotope does not significantly alter the intermolecular interactions, such experiments can yield the exchange rates at thermal equilibrium. One methodologically related example (but not so concerning the nature of the exchange process) is NMR studies of hydrogen exchange rates in proteins (2): These provide vital clues about protein structure and dynamics. Another example is the radiochemical investigation of ion exchange between the aqueous phase and the crystals in mineral suspension (3).

There are fewer examples for application of such techniques to the exchange between spatial domains that contain different macroscopic forms of the same molecule, such as exchange between crystals and solute in a saturated dispersion. Often, the exchange between dissolved and solid material occurs in an interfacial region through which the conditions vary continuously from solid to liquid. Dissolved components crystallize at the surface of the crystals, parallel to a process where the crystal surface redissolves into the continuous phase. These processes lead to recrystallization of the solid phase and may eventually change its structure or properties. Therefore, molecular exchange can be related to various aging processes in numerous applications.

In the field of lipids, there is to date only one such study (4) in a system containing TG. With tripalmitin (PPP) radiolabeled by ^{14}C as the probe, the exchange process between dissolved ^{14}C-PPP and unlabeled PPP crystals was monitored. However, the radiolabeling method produced some difficulties and errors due to temperature fluctuations out of the optimal temperature range. In this paper, we introduce instead an NMR technique to measure the exchange rates between liquid and solid phases of dispersed lipids. Owing to its experimental simplicity and its potential to follow the process *in situ*, this NMR technique seems to be superior to the previous radiolabeling method. NMR spectroscopy (typically ^{1}H) is frequently used for the determination of total solids content

*To whom correspondence should be addressed at YKI, Institute for Surface Chemistry, Box 5607, SE-114 86 Stockholm, Sweden.
E-mail: paul.smith@surfchem.kth.se

in oil mixtures (5–8), and ^{1}H NMR imaging has been applied to visualize crystallization in lipid dispersion (9–11). Deuterium (^{2}H) NMR also has been applied to characterize the molecular mobility in and the transitions between the α- and β-crystalline states of PPP (12).

EXPERIMENTAL PROCEDURES

Materials. (i) TG crystals. Pure PPP (>99%; Sigma, St. Louis, MO) was crystallized from hexane (PA quality) and carefully vacuum dried. As determined by DSC (DSC 821; Mettler Toledo), the PPP crystals were in the stable polymorphic form (β) with a m.p. of 66.4°C, in agreement with previously published data (7). The melting enthalpy obtained was 177 kJ/mol, which is slightly higher than the previously published value by Timms (13) of 171 kJ/mol but in full agreement with the value by van Miltenburg and ten Grotenhuis (14) of 177 kJ/mol. Light microscopy showed a typical crystal size of 20–60 μm. The surface area *A* of the crystals was determined as 2.077 m^2/g from krypton gas adsorption experiments using BET-isotherms.

(ii) Deuterated TG. Per-deuterated PPP (^{2}H-PPP, $C_{51}D_{98}O_6$; Larodan, Malmö, Sweden) was used as probe. The m.p. and the enthalpy of fusion of ^{2}H-PPP were determined by DSC as 64.5°C and approximately 179 kJ/mol, respectively. Note that the enthalpy of fusion obtained is about 2 kJ/mol higher than that of hydrogenated PPP. Eads *et al.* (12) observed melting at 66°C even for the fully deuterated PPP and a melting enthalpy of 172 kJ/mol, values that are comparable to the corresponding data for the nondeuterated material (see above). Thus, we conclude that the two materials are sufficiently similar to assume complete mixing even in the β-crystalline state.

To prove this latter point, DSC determinations and X-ray diffraction measurements were performed in samples of mixed (crystallized from mixed melt) crystals. DSC revealed no appreciable difference in the melting enthalpies of crystals of the mixed systems. X-ray diffraction showed lattice spacings independent of the proportion of deuterated material and identical to spacings obtained in β-form crystals of nondeuterated PPP. Moreover, we observed no duplication of the diffraction peaks. Thus, we can conclude that mixed β-polymorphs of hydrogenated and deuterated PPP are readily formed.

(iii) TG oil. A medium-chain TG oil (MCT; Karlshamns AB, Karlshamn, Sweden) was used as solvent for PPP. The oil contained 96.6% TG, 3.2% DG, <0.1% MG, and <0.1% FFA. The main FA in the MCT oil were caprylic acid (8:0, 61.8%) and capric acid (10:0, 37.6%).

Methods. (i) Preparation of the saturated solution. A saturated oil solution of PPP in MCT was prepared at the selected temperature (T = 40°C) by weighing the components together at the saturation mole fraction estimated from the standard expression (15),

$$X_{\text{sat}} = \exp\left\{-(H_m/R)\times\left[(T)^{-1} - (T_m)^{-1}\right]\right\} \quad [1]$$

where H_{m} is the enthalpy of fusion for PPP (177.2 kJ/mol), R is the universal gas constant, and T_m is the m.p. of PPP. PPP was added to the MCT oil at the concentration calculated from the estimated mole fraction $X_{\text{sat}} = 5.03 \times 10^{-3}$. The mixture was stirred and warmed to approximately 60°C until a clear and homogeneous solution was observed. After 10 min, the solution was cooled to 40°C and held at this temperature for at least 60 min. This solution was then used as the liquid phase in the experiments.

The exchange process between solute and solid PPP was detected *via* ^{2}H-PPP as probe in the liquid. Since the DSC analysis showed minor differences in the enthalpy of fusion and melting temperature between the labeled (^{2}H-PPP) and unlabeled (^{1}H-PPP) PPP, experiments were performed with the liquid phases saturated by PPP that contained different fractions of labeled PPP (10, 25, or 50% ^{2}H-PPP).

(ii) Preparation of the samples. A dispersion of TG crystals in oil was obtained by adding 1.50 mL of the saturated oil solution (liquid phase) to unlabeled PPP crystals held at 40°C in a 10-mm NMR tube. The dispersion was mixed for about 10 s using a vortex mixer and transferred quickly (within 30 s, during which the sample was thermally isolated) to an NMR instrument (Varian Unity Inova 500 MHz or Bruker AMX 300 MHz). The temperature in the NMR probe was preset to 40°C before inserting the sample. By repeated visual inspection, it was found that spinning samples in the NMR probe at a 25-Hz spinning rate prevented sedimentation of the crystals in the dispersion. This phenomenon is similar to the suppression of thermal convection by sample spinning (16). Hence, all experiments were performed under such spinning conditions.

(iii) NMR experiments. Nuclear spins are subject to different spin interactions, most of them anisotropic (17). Hence, in solid powders (in contrast to single crystals) the NMR spectra are usually broad. This is also the case for ^{2}H nuclei whose dominant spin interaction is the so-called quadrupole coupling that, for nuclei involved in C–^{2}H bonds of solid organic material, leads to a line broadening by ~10^5 Hz (18). On the other hand, fast and isotropic molecular motions in liquids lead to an averaging of the anisotropic spin interactions with the result of narrow (typically ~1 Hz) NMR lines. Hence, the spectral contribution from solids is effectively cancelled in NMR spectra recorded under "high-resolution" conditions. On the other hand, the signal from nuclei residing in liquids is conveniently detected. Indeed, the lack of an NMR signal from solid ^{2}H-PPP powder was tested to be complete when recorded in high-resolution multinuclear NMR probes and with the selected 10-kHz spectral width. This forms the basis of our method where the integral intensity of the recorded ^{2}H NMR spectra measures the amount of ^{2}H nuclei and, hence, ^{2}H-PPP in the liquid phase.

After placing the sample into the NMR probe, ^{2}H spectra were recorded at regular intervals (every 6 or 13 min). The signal was typically obtained by averaging 128 scans with a few seconds or minutes of recycling delay. Note that the longitudinal relaxation time T_1 of ^{2}H in PPP was about 300 ms. The absolute amount of ^{2}H-PPP could then be obtained by

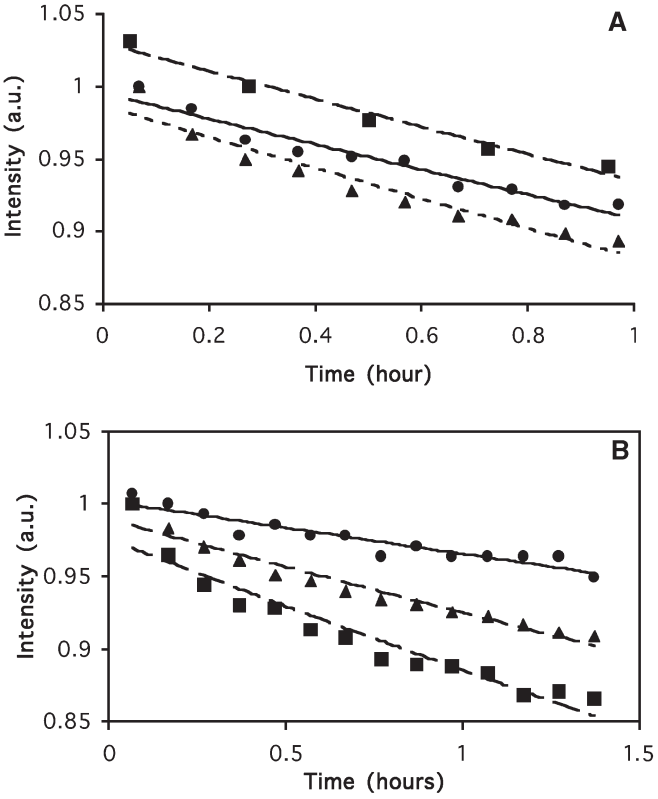

FIG. 1. Normalized ^{2}H spectral intensities (see text) in the first 80 min of the exchange experiments. The decay rates *r* obtained by least-square fitting (fitted decays shown by lines) are presented in Table 1. (A) Data obtained in experiments with different fractions of the ^{2}H-labeled PPP in the liquid phase of 1.50 mL MCT oil saturated by PPP: (●) solid line, 10% ^{2}H-PPP in solution with 44.7 mg ^{1}H-PPP crystals added; (▲) dashed line, 25% ^{2}H-PPP in solution with 41.1 mg ^{1}H-PPP crystals added; (■) dash-dotted line, 50% ^{2}H-PPP in solution with 42.7 mg ^{1}H-PPP crystals added). (B) Data obtained in experiments with different amounts of ^{1}H-PPP crystal immersed in a solution of 1.50 mL MCT oil saturated by PPP containing 25% ^{2}H-PPP: (●) solid line, 23.3 mg; (▲) dashed line, 30.9 mg; (■) dash-dotted line, 55.5 mg. MCT, medium-chain TG; PPP, tripalmitin.

comparing the intensity of the signal (I_{PPP}) to that yielded by a reference sample containing MCT oil with an equal amount of ^{1}H-PPP in it (I_{ref}). The spectrum recorded in the reference sample arose from ^{2}H nuclei at natural abundance (0.015%). For the present experiment, however, it sufficed to record the relative variation of $I(t) = I_{PPP}(t) - I_{ref}$ with time, counted from the preparation of the dispersion. Such data for several of the experiments are presented in Figure 1.

RESULTS AND DISCUSSION

The exchange process for which we are aiming here is assumed to be a molecular exchange at the liquid–solid interface. The exchange rate is followed by adding unlabeled ^{1}H-PPP crystals to a saturated solution with a known fraction of ^{2}H-PPP in the solution. The exchange reaction is manifested as a loss of ^{2}H-PPP in the liquid, which is clearly shown by the decreasing ^{2}H NMR intensity (Fig. 1). Since the NMR tube is a closed system, all ^{2}H-PPP molecules that leave the liquid phase must form part of the solid phase.

We apply a simple description of the equilibrium exchange rate by assuming a constant precipitation/crystallization (k_1) and a constant dissolution (k_2) rate. The reaction is assumed to be surface specific; thus, the rates k_1 and k_2 can be expressed as molar or mass units per unit area and time and represent the diffusive flow in and out over the phase boundary

$$[\mathrm{PPP}]_{\mathrm{liquid}} \underset{k_2}{\overset{k_1}{\rightleftharpoons}} [\mathrm{PPP}]_{\mathrm{solid}} \qquad [2]$$

At equilibrium the crystallization of dissolved PPP (both labeled and unlabeled) onto the added PPP crystals occurs at the same molecular rate as the dissolution of PPP from the crystals into the liquid. Hence, the liquid phase remains saturated. The exchange rate, k_1 and k_2, can be assumed to be constant (as long as the particle size is unaltered). If the loss of ^{2}H-PPP from solution obeys a first-order reaction in the system containing a fraction of ^{2}H-PPP dissolved in the liquid phase, the loss of ^{2}H-PPP, as a result of the exchange process, should be directly proportional to its concentration. In fact, as shown in Figure 2, this is the case. Hence, the loss of ^{2}H-PPP from the solution should be described by a first-order reaction.

In the actual setup, the PPP crystals initially contained only unlabeled PPP, and because ^{2}H-PPP precipitates slowly on the surface of the PPP crystals, the rate of redissolution of ^{2}H-PPP back into the liquid is negligible. Therefore, process k_2 initially can be neglected for ^{2}H-PPP, yielding

$$d\left[{}^2\mathrm{H} - \mathrm{PPP}_{\mathrm{liquid}}\right] = -r\left[{}^2\mathrm{H} - \mathrm{PPP}_{\mathrm{liquid}}\right] \cdot dt \qquad [3]$$

solution of which provides

$$\ln\left\{\frac{\left[{}^2\mathrm{H} - \mathrm{PPP}_{\mathrm{liquid}}\right]_t}{\left[{}^2\mathrm{H} - \mathrm{PPP}_{\mathrm{liquid}}\right]_0}\right\} = r \cdot t \qquad [4]$$

The actual rate can then be obtained by fitting an exponential function to the time-dependent experimental intensities. From

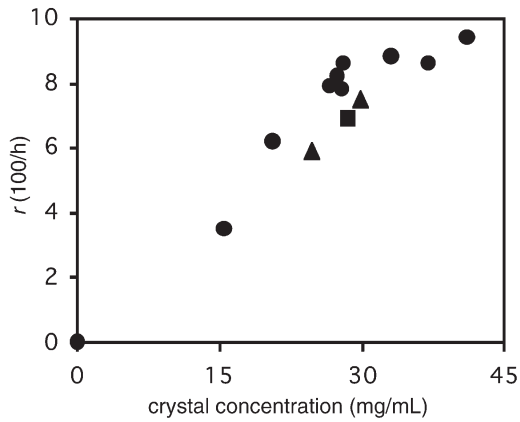

FIG. 2. The absolute exchange rate, *r*, as a function of the crystal concentration. All experiments in Tables 1 and 2 are included. Experiments using different fractions of deuterium-labeled PPP are indicated: (25% deuterium labeled ●, 10% labeled ▲, and 50% labeled ■).

the data, some sets of which are presented in Figure 1, the rate of the decrease of ^{2}H-PPP concentration r was extracted by least-squares fitting of an exponentially decaying function of time t, $f(t) = I(0)* \exp(-rt)$ with zero-time intensity of the ^{2}H signal $I(0)$ as free parameter (note that the first intensity data are recorded a few minutes after preparing the dispersion; see above). The fitting is performed within a rather limited range, typically within less than 20% reduction of the signal. Hence, the deviation from linearity is small. The reason for limiting the time of the experiments is to be able to assume a constant specific area (small effects due to Ostwald ripening) and to neglect the dissolution flow k_2.

To extract k (= k_1) from r, three observations must be made. First, r (in units of time^{-1}) characterizes the relative variation of the amount of ^{2}H-PPP in the liquid. Second, although the decrease of the ^{2}H signal intensity measures only the amount of ^{2}H-PPP crystallized from the liquid onto the solid, ^{1}H-PPP molecules are also crystallized at the same rate. Hence, to obtain the specific rate, one must multiply r by the total initial PPP concentration/unit volume of the liquid. Third, the specific exchange rate per unit surface k is obtained by normalizing with the surface area of crystals per unit volume A. This, in principle, requires that all faces are active in the exchange process. However, relative comparisons can be made as long as we operate under conditions where the active surface fraction can be assumed to be constant. Hence, the surface specific exchange rate k is obtained as

$$k = r \cdot \frac{[\mathrm{PP}P]_{\mathrm{liquid}}}{A} \qquad [5]$$

with the equilibrium solubility $[\mathrm{PPP}]_{\mathrm{liquid}} = 7.76$ mg/mL (corresponding to $X_{\mathrm{sat}} = 5.03 \times 10^{-3}$ as estimated in the Methods section) and the specific area $A' = 2.08$ m^2/g (see the Materials section).

There are two types of random error, the scatter of the measured NMR intensities for a particular sample and the variation between experiments performed on separately prepared samples. The error of r, obtained in a single sample and reported to one SD, has been extracted from the scatter of the experimental NMR intensity points around the fitted curve (19).The stochastic errors of the experimental setup have been tested by repeated experiments with approximately 30 mg/mL added PPP crystals. The results, given in Table 1, show the scatter in the exchange rates obtained. The SD between the experiments is 0.36, which is somewhat below the error of individual r estimates (see above). Thus, we may conclude that the between-experiment variation does not contribute significantly to the errors and that the error estimation from the slope gives a fair description of the uncertainty of the method.

We have postulated that the exchange rate is a surface-determined reaction. Therefore, the amount of crystals in the samples was varied with the objective of verifying the method and the theory. The results are shown in Table 2. In Figure 2 the absolute exchange rate, r, is given as a function of the amount of added crystal, showing an acceptable linear correlation (correlation factor 0.87). Thus, it is clear that the results agree with a surface-determined reaction. However, it is also clear that the specific exchange rates obtained at high (above 35 mg/mL) and low (below 20 mg/mL) crystal concentrations are significantly different from the rates obtained at intermediate concentrations. This might be a consequence of (i) a stronger tendency toward sedimentation at lower crystal concentrations, and (ii) difficulty in wetting all crystals at higher crystal concentrations, both of which may result in an inhomogeneous system with poor equilibration. Thus, acceptable limits of the validity of the experimental method are obtained.

TABLE 1
Exchange Rate, *r, for* 25% Fraction of ^{2}H-PPP in the Liquid Phase and with Added Crystals in the Vicinity of 27 mg/mL[a]

Mass of added ^{1}H-PPP crystals, M (mg/mL)	r (10^2/h)	τ (h)	A (10^2/m)	Specific exchange rate k [mg/(h·m^2)]
27.4	8.2 ± 0.4	8.4 ± 0.4	570	11.2 ± 0.6
26.6	7.9 ± 0.4	8.8 ± 0.5	553	11.1 ± 0.6
28.1	8.6 ± 0.7	8.1 ± 0.7	584	11.4 ± 0.9
27.9	7.8 ± 0.4	8.9 ± 0.5	580	10.4 ± 0.6
SD[b]				0.36

[a]The error of *r,* given to one SD, has been obtained from the scatter of the experimental points around the fitted curve as described in the text. The half-life time τ is calculated as $\tau = \ln 2/r$. The specific exchange rate k has been obtained from r and A *via* Equation 5.
[b]This SD reflects the between-experiment variation of r obtained in separately prepared samples. Abbreviation: *A,* surface area of crystals per unit volume.

The random error due to scattering of the data points increases when the amount of added crystals is less than about 20 mg/mL; this is partly a consequence of the smaller relative variation of the signal intensity. Nevertheless, the specific exchange rates obtained at different PPP crystal contents in the dispersions (an almost threefold variation of 15–40 mg PPP crystals per mL) are reasonably close (within a range of ±30%) to each other. As seen in Table 2 and Figure 2, the specific exchange rates obtained with different mole fractions (10, 25, and 50%) of ^{2}H-PPP in the liquid phase do not significantly differ. This proves that the minor differences (see above) in molecular properties between labeled and unlabeled PPP do not affect the results.

To prove this point further, we also performed an experiment in a reverse setup where fully deuterated PPP crystals (*ca.* 30 mg/mL, instead of hydrogenated PPP) were immersed into the saturated (with 25% ^{2}H-PPP and 75% ^{1}H-PPP) liquid phase. From the subsequent increase of the ^{2}H NMR signal, k was estimated to 11.1 ± 0.6 mg/h·m^2.

Some molecular features are important regarding the nature of the exchange process. Recall that our objective was to characterize the precipitation–dissolution equilibrium between the crystals and the surrounding liquid and the gradual inclusion of previously dissolved material into the crystals. An alternative explanation of the experimental observations is the formation of an adsorbed layer of PPP at the surface of the added crystals; hence, the data would characterize adsorp-

TABLE 2
Exchange Rate, *r*, for Different Fractions of ^{2}H-PPP in the Liquid Phase and with Different Amounts of Added Crystal[a]

Fraction of ^{2}H-PPP in MCT (%)	Mass of added ^{1}H-PPP crystals, M^b (mg/mL)	r (10^2/h)	τ (h)	A^b (10^2/m)	Specific exchange rate k [mg/(h·m^2)]
25	15.5	3.5 ± 0.5	19.8 ± 2.8	323	8.4 ± 1.2
25	20.6	6.2 ± 0.3	11.2 ± 0.5	427	11.3 ± 0.6
25	*27.5*				*11.0 ± 0.4*[c]
25	33.1	8.8 ± 0.5	7.9 ± 0.6	689	9.9 ± 0.6
25	37.0	8.6 ± 0.6	8.1 ± 0.6	768	8.7 ± 0.6
25	41.1	9.4 ± 0.8	7.4 ± 0.6	853	8.6 ± 0.7
10	24.6	5.9 ± 0.4	11.8 ± 0.8	511	9.0 ± 0.6
10	29.8	7.5 ± 0.4	9.2 ± 0.5	619	9.4 ± 0.5
50	28.5	6.9 ± 1.0	10.0 ± 1.5	591	9.1 ± 1.3

[a]Values derived from the data, some sets of which are presented in Figure 1. The error of *r,* given to one SD, has been obtained from the scatter of the experimental points around the fitted curve as described in the text. The half-life time τ is calculated as τ = ln2/*r*. The specific exchange rate *k* has been obtained from *r* and *A via* Equation 5.
[b]The error of these quantities is small compared to the error in *r*.
[c]The average of results presented in Table 1, with the error limit representing the total estimated error originating from both the systematic spread (Table 1) and the random scatter (19). MCT, medium-chain TG; for other abbreviation see Table 1.

tion kinetics. However, this possibility can be excluded for two reasons. (i) PPP cannot be expected to display large surface activity in a TG solution (such as the MCT oil). Measurements by Johansson and Bergenståhl (20) of adsorption of acylglycerols at TG crystals dispersed in a liquid TG show that such adsorption is weak and results in thin layers. (ii) The exchange process proceeds without a change in kinetics over time, allowing for an exchange of more material than in a monolayer. Furthermore, the same *k* value was obtained in the reverse setup (see above), which is not at all sensitive to any eventual adsorption.

The sample with crystal content of 27 mg/mL corresponds to a specific surface of 0.05 m^2/mL. The amount of dissolved PPP is about 8 mg/mL. A monolayer of PPP at the surface corresponds to 3 mg/m^2, giving 0.15 mg/mL, which is about 2% of dissolved PPP. The experiments proceeded until about 10% of the ^{2}H-PPP had been lost from the solution (0.8 mg/mL), which means that 4% of the ^{1}H-PPP originally in the crystal was replaced with ^{2}H-PPP and ^{1}H-PPP from the liquid. This 0.8 mg/mL corresponds to 15 mg/m^2 crystal, which is approximately three to four molecular layers of PPP. The observation that the exchange process continues with first-order kinetics over a time scale corresponding to more than a fraction of a monolayer suggests that the process originates from precipitating and dissolving faces of the crystals.

The precipitation–dissolution equilibrium between the crystals and the surrounding liquid may alter the size distribution of the crystals in the sample *via* Ostwald ripening (21,22). If this process proceeded longer, we could expect a loss of area due to the growth of larger and shrinkage of smaller particles. However, in the short experimental time scale used here, the changes in the total interfacial area can be neglected.

The diffusion of dissolved PPP ($D > 10^{-11}$ m^2/s) over the length scale of 100 μm (average liquid domain size) leads to an average diffusion time in the order of $t_d < 10^3$ s << τ, the half-life time (see Tables 1 and 2). Hence, the observed exchange is not limited by bulk diffusion (22) but entirely by surface mechanisms.

The NMR procedure presented here allows a direct *in situ* measurement of the exchange between solid and liquid phases and thereby provides a new source of information about crystal–solvent interfaces. The method does not demand any separation step, unlike the previously published method (4) based on ^{14}C-labeled material. A separation procedure suffers from serious limitations that are due to the difficulties of maintaining constant conditions. We note particularly that the solid–liquid equilibrium is extremely sensitive to variations in temperature.

Attention must be called to two specific limitations of the NMR method. First, at low saturation levels where the signal intensity from the deuterated probe is comparable to the natural ^{2}H background signal, the experiment cannot provide accurate exchange rates because the NMR signal does not measure the probe concentration well. In the present system this limits from below the temperature range over which the PPP exchange rates can be measured. Second, at high saturation levels the fractional change of probe concentration due to exchange is small because the absolute number of dissolved PPP molecules is high. This effect limits the accessible temperature range from above. We estimate that, in the present dispersion, NMR cannot provide accurate exchange rates out of the 25–50°C ranges for PPP in oil.

All similar exchange experiments performed in dispersions face another problem: dissolution and precipitation may vary from one crystal plane to another. Hence, some surfaces of a grain may grow more while others may shrink. The method presented here does not address such variation.

ACKNOWLEDGMENTS

The authors are grateful to Jari Alander (Karlshamns AB, Sweden) for valuable discussions. We thank Charlotta Damberg (Swedish NMR Center, Gothenburg University, Gothenburg, Sweden) and Hans Ringblom (YKI) for assistance. The "Future Technologies for Food Production Program" (LiFT) and Karlshamns AB and the Swedish Natural Science Research Council (NFR) are gratefully acknowledged for financial support.

REFERENCES

1. Sato, K., S. Ueno, and J. Yano, Molecular Interactions and Kinetic Properties of Fats, *Progress Lipid Res. 38*:81–116 (1999).
2. Raschke, T.M., and S. Marqusee, Hydrogen Exchange Studies of Protein Structure, *Curr. Opinion Biotechnol. 9*:80–86 (1998).
3. Das, H.A., and R.D. Van Der Weyden, Isotopic Exchange Measurements in Batch Adsorption and Desorption Measurements, *J. Radioanal. Nucl. Chem. 191*:229–238 (1995).
4. Haghshenas, N., P. Smith, and B. Bergenståhl, The Exchange Rate Between Dissolved Tripalmitin and Tripalmitin Crystals, *Colloids Surf. B 21*:239–243 (2001).
5. Mansfield, P.B., A New Wide-Line NMR Analyzer and Its Use in Determining the Solid–Liquid Ratio in Fat Samples, *J. Am. Oil Chem. Soc. 48*:4–6 (1971).
6. Haighton, A.J., L.F. Vermaas, and C. den Hollender, Determination of the Solid–Liquid Ratio of Fats by Wide-Line Nuclear Magnetic Resonance, *Ibid. 48*:7–10 (1971).
7. van Putte, K., L. Vermaas, J. van den Enden, and C. den Hollander, Relationship Between Pulsed NMR, Wide-Line NMR and Dilatometry, *Ibid. 52*:179–181 (1975).
8. Norris, R., and M.W. Taylor, Comparison of NMR and DSC Methods for the Estimation of Solid Fat Content, *N.Z. J. Dairy Sci. Technol. 12*:160–165 (1977).
9. Simoneau, C., M.J. McCarthy, R.J. Kauten, and J.B. German, Crystallization Dynamics in Model Emulsions from Magnetic Resonance Imaging, *J. Am. Oil Chem. Soc. 68*:481–487 (1991).
10. Simoneau, C., M.J. McCarthy, D.S. Reid, and J.B. German, Influence of Triglyceride Composition on Crystallization Kinetics of Model Emulsions, *J. Food Eng. 19*:365–387 (1993).
11. Ozilgen, S., C. Simoneau, J.B. German, M.J. McCarthy, and D.S. Reid, Crystallization Kinetics of Emulsified Triglycerides, *J. Sci. Food Agric. 61*:101–108 (1993).
12. Eads, T.M., A.E. Blaurock, R.G. Bryant, D.J. Royand, and W.J. Croasmun, Molecular Motion and Transitions in Solid Tripalmitin Measured by Deuterium Nuclear Magnetic Resonance, *J. Am. Oil Chem. Soc. 69*:1057–1068 (1992).
13. Timms, R.E., Heats of Fusion of Glycerides, *Chem. Phys. Lipids 21*:113–129 (1978).
14. van Miltenburg, J.C., and E. ten Grotenhuis, A Thermodynamic Investigation of Tripalmitin. Molar Heat Capacities of the α- and β-Form Between 10 K and 350 K, *J. Chem. Eng. Data 44*: 721–726 (1999).
15. Atkins, P.W., *Physical Chemistry*, 6th edn., Oxford University Press, Oxford, United Kingdom, 1998.
16. Lounila, J., K. Oikarinen, P. Ingman, and J. Jokisaari, Effects of Thermal Convection on NMR and Their Elimination by Sample Rotation *J. Magn. Reson. A 118*:50–54 (1996).
17. Abragam, A., *The Principles of Nuclear Magnetism*, Clarendon, Oxford, United Kingdom, 1961.
18. Schmidt-Rohr, K., and H.W. Spiess, *Multidimensional Solid-State NMR and Polymers*, Academic Press, London, 1994.
19. Press, W.H., B.P. Flannery, S.A. Teukolsky, and W.T. Vetterling, *Numerical Recipes*, Cambridge University Press, Cambridge, United Kingdom, 1986.
20. Johansson, D., and B. Bergenståhl, The Influence of Food Emulsifiers on Fat and Sugar Dispersions in Oils. 1. Adsorption, Sedimentation, *J. Am. Oil Chem. Soc. 69*:705–717 (1992).
21. Lifshitz, I.M., and V.V. Slyozov, The Kinetics of Precipitation from Supersaturated Solid Solutions, *J. Phys. Chem. Solids 19*:35–50 (1961).
22. Mullin, J.W., *Crystallization*, 4th edn., Butterworth-Heinemann, Oxford, United Kingdom, 2001.

[Received June 26, 2003; accepted September 11, 2003]